Semiconductor Science and Technology

PAPER

# Low-leakage kV-class GaN vertical p–n diodes with non-destructive breakdown enabled by hydrogen-plasma termination with p-GaN extension

To cite this article: Chen Yang *et al* 2021 *Semicond. Sci. Technol.* **36** 075009



IOP Publishing Semiconductor Science and Technology
Semicond. Sci. Technol. **36** (2021) 075009 (6pp) https://doi.org/10.1088/1361-6641/ac038f

# Low-leakage kV-class GaN vertical p–n diodes with non-destructive breakdown enabled by hydrogen-plasma termination with p-GaN extension

**Chen Yang[1], Houqiang Fu[2,*], Kai Fu[1], Tsung-Han Yang[1], Jingan Zhou[1], Jossue Montes[1] and Yuji Zhao[1,*]**

[1] School of Electrical, Computer and Energy Engineering, Arizona State University, Tempe, AZ 85287, United States of America
[2] Department of Electrical and Computer Engineering, Iowa State University, Ames, IA 50011, United States of America

E-mail: houqiang@iastate.edu and yuji.zhao@asu.edu

Received 7 March 2021, revised 17 May 2021
Accepted for publication 20 May 2021
Published 7 June 2021

**Abstract**

This paper demonstrates low-leakage hydrogen plasma (HP) terminated GaN-on-GaN vertical p–n diodes. The leakage current was decreased by ∼800 times (at −600 V), and the breakdown voltage was nearly doubled with a p-GaN extension design. The devices showed a non-destructive breakdown voltage of 1.68 kV, a specific on-resistance ($R_{on}$) of 0.40 MΩ cm$^2$, and a Baliga's figure of merit of 7.1 GW cm$^{-2}$. These results indicate that HP termination with p-GaN extension is effective in reducing leakage and enhancing the breakdown capability of vertical GaN power diodes.

Keywords: gallium nitride, vertical power diodes, edge termination, leakage, breakdown, power electronics

(Some figures may appear in color only in the online journal)

Vertical GaN power devices have attracted extensive research over the past several years due to the availability of high-quality bulk GaN substrates [1–3]. The edge termination techniques are critical in GaN power electronics to reduce leakage and prevent premature device breakdown. One of the most commonly reported methods is mesa termination via dry etching, including beveled mesas [4], multi-step mesas [5, 6], and deep mesas [7]. Mesa termination is also often used in combination with field plates (FPs). However, the p-GaN is sensitive to dry etching, which can induce etching damages and trap states that are difficult to be recovered [8]. Sugimoto *et al* [9] reported that the mesa sidewall p-GaN surface could be transformed into depleted p-GaN or n-GaN, which could induce leakage current under high reverse bias. Furthermore, the mesa termination requires precise control of etching angles and mesa steps via many factors such as etching mask, inductively coupled plasma (ICP) power, and radio frequency (RF) power, ratios of mixed gas, flow rate and chamber pressure, etc [10], thus complicating the fabrication process. Another common edge termination approach is ion implantation. Although this technique has been widely used in SiC power devices, it is still under development and far from mature for GaN devices [11–14], especially for p-GaN implantation.

To overcome these challenges, some researchers have demonstrated a plasma-based edge termination technique for GaN devices [15, 16], such as hydrogen and nitrogen plasma. The hydrogen atoms and Mg can form neutral complexes, which transform the p-GaN into high resistive GaN (HR-GaN) without introducing damages or defects. This method is easy to implement and enables an etching-free and implantation-free process for GaN power diodes. GaN power diodes

* Authors to whom any correspondence should be addressed.

 

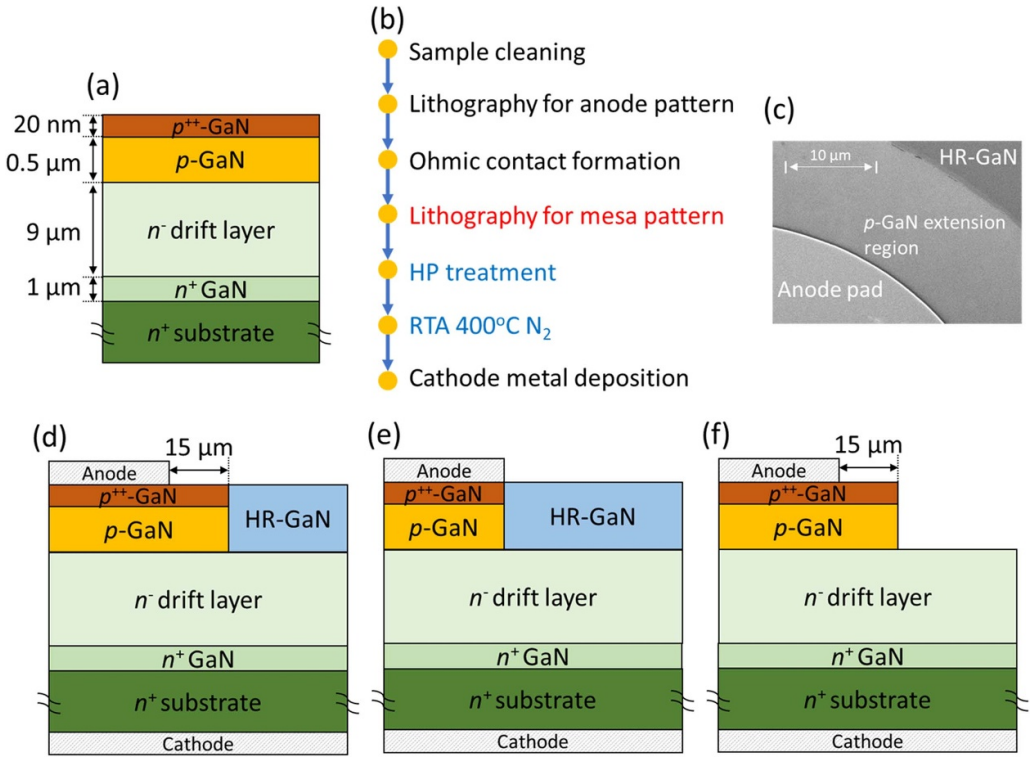


**Figure 1.** (a) The schematic of the GaN p–n diode epilayers. (b) Device fabrication process. (c) SEM image of the p-GaN extension region. The schematics of the devices with different edge terminations: (d) HP w/p-GaN extension, (e) HP w/o p-GaN extension, and (f) mesa etch.

with hydrogen plasma (HP)-based edge termination [17] and guard ring structures [18] showed good device performance. Although high breakdown voltages were achieved in the previous plasma terminated diodes [16–18], they still presented a catastrophic breakdown and a high level of reverse leakage due to the unoptimized edge termination design. During fabrication of the edge termination, the hydrogen atoms may diffuse underneath the electrodes, which may introduce serious leakage issues. However, the reverse leakage characteristics of vertical GaN power diodes with HP edge termination have not been thoroughly studied. In this work, we optimized the HP edge termination with a p-GaN extension region and comprehensively studied the leakage characteristics of the HP-terminated GaN vertical p–n diodes. This design significantly decreased the leakage current and improved the breakdown performance of the devices.

GaN p–n diode epilayers were grown on free-standing GaN substrates by metalorganic chemical vapor deposition. The substrate was provided by Sumitomo Corporation grown by hydride vapor phase epitaxy. The threading dislocation density of the substrate was $\sim 10^6$ cm$^{-2}$, and the carrier concentration of the substrate was $\sim 10^{18}$ cm$^{-3}$. An 1-$\mu$m-thick n$^+$-GaN ([Si] $= 2 \times 10^{18}$ cm$^{-3}$) layer was first grown on the substrate, followed by a 9-$\mu$m-thick unintentionally doped (UID) drift layer, a 0.5-$\mu$m-thick p-GaN ([Mg] $= 10^{19}$ cm$^{-3}$) and finished by a 20-nm p$^{++}$-GaN ([Mg] $= 10^{20}$ cm$^{-3}$) for the ohmic contact, as shown in figure 1(a). The average carrier concentration of the UID-GaN drift layer was $\sim 5 \times 10^{15}$ cm$^{-3}$ as determined by capacitance–voltage ($C$–$V$) measurements [16].

The device fabrication process flow for the GaN p–n diodes is presented in figure 1(b). The samples were first cleaned in acetone and isopropyl alcohol by ultrasonic and then rinsed with deionized water. Conventional photolithography was used for the formation of anode patterns. Metal stacks of Pd/Ni/Au were then deposited by electron beam evaporation. The diameter for the anode electrode is 70 $\mu$m. The mesa patterns were then formed by photolithography and aligned to the metal contacts. It should be noted that the radius of the circular mesa patterns is 15-$\mu$m longer than that of the anode, creating a p-GaN extension region, as shown in figure 1(c). The exposed p-GaN was treated with HP generated by a PlasmaTherm Apex ICP system with ICP power of 300 W and RF power of 10 W for 5 min. A subsequent rapid thermal annealing treatment at 400 °C in $N_2$ for 5 min was applied to drive the hydrogen atoms deep into p-GaN and facilitate the formation of the Mg–H complexes. Finally, the cathode metal stacks of Ti/Au were deposited on the backside of the wafer. The schematic of the devices is illustrated in figure 1(d).

For comparison, two other types of devices with different edge terminations were also fabricated on the same wafer. In figure 1(e), the anode metals were used as self-aligned masks in the HP process, which is an unoptimized conventional design. In figure 1(f), mesa termination by ICP dry etching was used for the edge termination. The mesa depth is equal to the p-GaN thickness. The three devices are denoted as HP w/p-GaN extension, HP w/o p-GaN extension, and mesa etch devices, respectively, in this paper. No FPs and passivation were used in this work. The forward and reverse $I$–$V$ curves

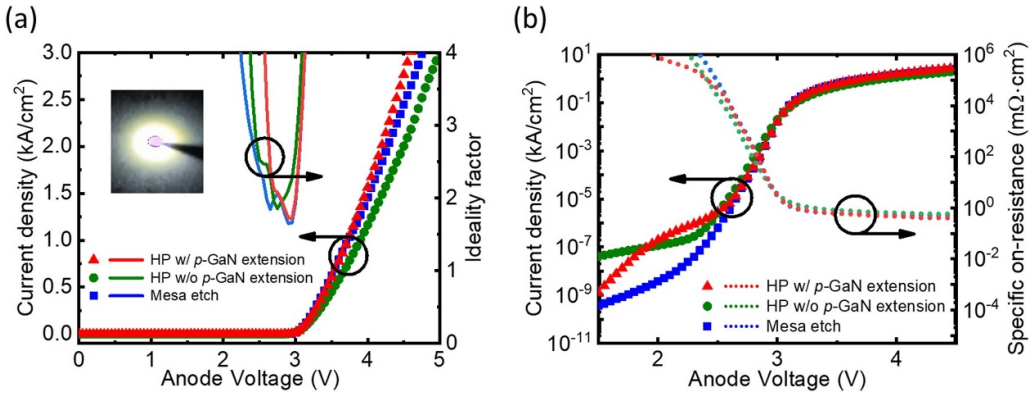


**Figure 2.** Device forward characteristics: (a) current density and ideality factors at forward bias in linear scale (inset: electroluminescence of devices under forward bias). (b) Current density and specific on-resistance at forward bias in semi-log scale.

were measured by a Keithley 2657A source meter. Breakdown measurements were conducted with samples immersed in Fluorinert FC-70 to avoid electrical flash-over in the air.

Figure 2(a) presents the forward *I*–*V* characteristics and ideality factors of the three devices. The current density was normalized by the anode area. The HP w/p-GaN extension device and mesa etch device show slightly higher on-current density as compared to the HP w/o p-GaN extension device. This is because the extended active p-GaN regions lead to current spreading in those two devices. The minimum ideality factors of the three devices were 1.7, 1.8, and 1.6, respectively. At forward bias, strong light emission was observed in all three devices (figure 2(a) inset). The strong electroluminescence is due to the radiative recombination of injected electrons and holes in the junction, which indicates the good material quality of the samples. Figure 2(b) shows the forward characteristics and specific on-resistance ($R_{on}$) in a semi-log scale. The $R_{on}$ of the three devices were 0.40, 0.43 (0.82 and 0.90 m$\Omega$ cm$^2$ if normalized by the total active region), and 0.44 m$\Omega$ cm$^2$, respectively. By linear extrapolation, the turn-on ($V_{on}$) voltages of the three devices were extracted as 3.3, 3.2, and 3.2 V, respectively. The three devices show very similar forward characteristics, which is beneficial for a fair comparison of breakdown voltages and reverse leakage currents.

Figure 3 shows the representative reverse *I*–*V* curves of the three devices. During the reverse *I*–*V* characteristics, an 1 $\mu$A compliance current was set to protect the sample and equipment. The breakdown voltages in these measurements were defined as the voltage where the reverse current reached the compliance current. The breakdown voltages of the three devices were 1.68, 0.79, and 1.24 kV, respectively. And the reverse leakage of the three devices at −600 V were 0.4, 333, and 52 nA, respectively. Compared with the HP w/o p-GaN extension device, the device with the p-GaN extension showed a significant reduction in reverse leakage current by over 800 times and a dramatic increase in device breakdown capability. The HP w/p-GaN extension device also showed improved performance compared with the mesa etch device. The lower performance of the mesa etch device is likely caused by dry etching-induced sidewall defects and damages [8, 9]. Furthermore, the breakdown for the two devices with HP-based edge

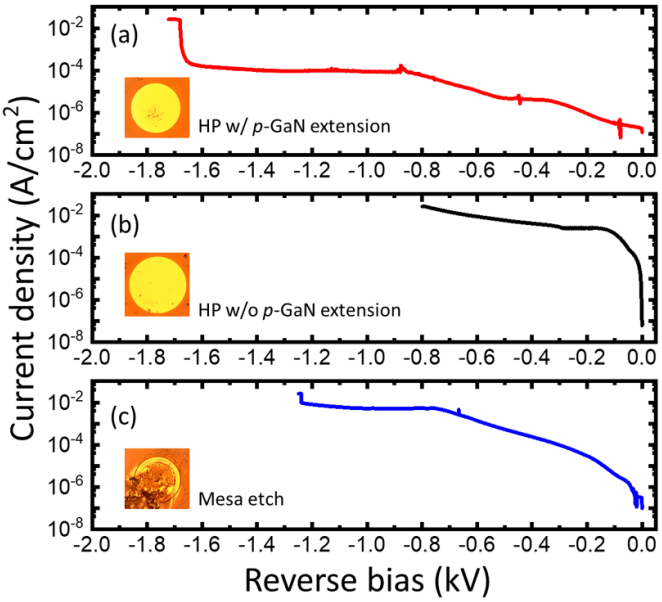


**Figure 3.** Reverse *I*–*V* characteristics for the three devices with different edge terminations. The insets show optical images of the three devices after breakdown.

termination was non-destructive, while the device with mesa etch termination showed hard breakdown with catastrophic damage of the anode metal.

In punch-through structures, the critical electric field ($E_c$) can be calculated with the following equation:

$$\mathrm{BV} = E_c d - \frac{eN_D d^2}{2\varepsilon_r \varepsilon_0} \tag{1}$$

where the $d$ and $N_D$ are the thickness and electron concentration of the GaN drift layer, the $\varepsilon_r$ is the relative permittivity of GaN, and $\varepsilon_0$ is the vacuum permittivity. The calculated $E_c$ for the three devices were 2.32, 1.33, and 1.83 MV cm$^{-1}$, respectively. The HP with p-GaN extension devices yielded the highest critical electric field of 2.32 MV cm$^{-1}$, which is also among the best values ever reported for the GaN vertical diodes [19].

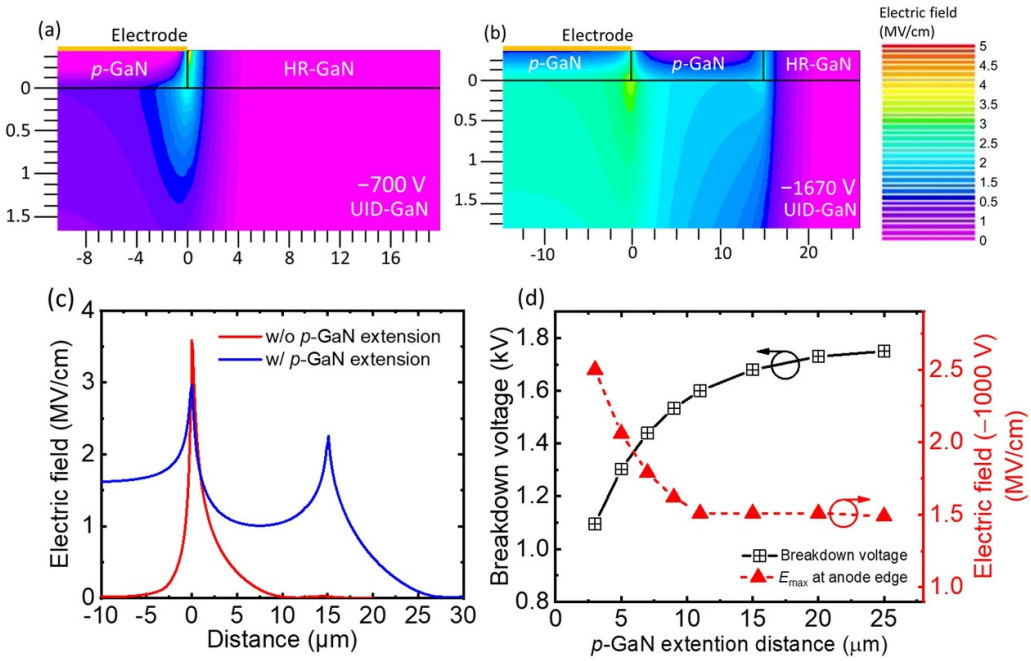


**Figure 4.** Simulated electric field distributions of devices with HP-based edge terminations at their breakdown voltages: (a) w/o p-GaN extension (−700 V) and (b) w/p-GaN extension (−1670 V). (c) Electric field distribution along horizontal cutline in the middle of p-GaN in the two devices. (d) Change of breakdown voltage and peak electric field at anode edge with the p-GaN extension distance at −1000 V.

To understand the effects of p-GaN extension, the devices with and without p-GaN extension were simulated using TCAD Silvaco. The electric field distributions and their breakdown voltages were calculated using the impact ionization model. The carrier concentrations for the p-GaN and UID-GaN were set as $2 \times 10^{17}$ cm$^{-3}$ and $5 \times 10^{15}$ cm$^{-3}$, respectively. According to [20], the electrical property of HR-GaN is close to an intrinsic semiconductor; therefore, we treated the HR-GaN as undoped GaN in this simulation for simplification. More factors such as trap related defects should be considered for more accurate simulation. For the HP w/o p-GaN extension device, the high electric field was concentrated around the anode edge close to the surface inside the HP-passivated p-GaN, which can become a breakdown 'hotspot'. Previous studies showed that the passivated p-GaN would allow for electrons tunneling at high field [20]. Without the p-GaN extension region, the electrons at the anode edge can directly tunnel through the HR-GaN, which induces large leakage in the HP w/o p-GaN extension device. For devices with p-GaN extension, the anodes were separated from HR-GaN, thus preventing the formation of tunnel current.

The HP w/p-GaN extension device (figure 4(b)) showed a much more uniform distribution of electric fields. The peak electric field was found inside the p-GaN instead of HP passivated p-GaN. The peak electric field in HP w/p-GaN extension device (figure 4(c)) is also largely reduced with two electric field peaks. In figure 4(d), with the increase of the p-GaN extension distance, the breakdown voltage increased, and the peak electric field at the anode edge under the same reverse bias (−1000 V) was reduced. The changes in the breakdown voltage and electric field were more rapid at small extension distance and gradually slowed down at higher values.

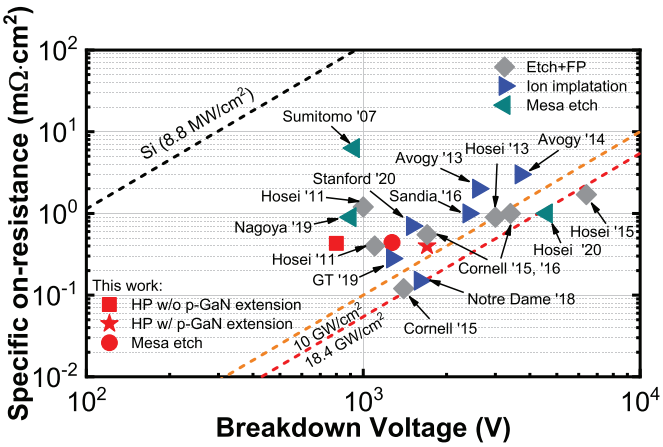


**Figure 5.** Benchmark of $R_{on}$ versus breakdown voltage of vertical GaN-on-GaN p–n diodes in [4, 6, 7, 14, 19, 21–31]. The shape of data points represents edge termination methods. The institute and publication year are also labeled.

The devices in this work are compared with the state-of-the-art devices with other edge termination technologies: etch + FP [4, 21–26], ion implantation [14, 19, 27–30], and mesa etch [6, 7, 31] in a benchmark plot (figure 5). The HP w/p-GaN extension devices with 1.68 kV/0.4 mΩ cm$^2$ are among the best reported GaN diodes, although they only have a drift layer of 9 $\mu$m and have no passivation or FPs. The leakage current level before the breakdown of this device is below $10^{-4}$ A cm$^{-2}$ (3.8 nA), which is also comparable to the reported avalanche diodes [21]. These results show that by introducing a p-GaN extension region, the performance of HP-terminated GaN p–n diodes can be significantly improved.

In summary, low-leakage kilovolt-class GaN-on-GaN vertical p–n diodes were fabricated by hydrogen-plasma termination. The leakage current of hydrogen-plasma terminated devices was studied. The devices with a p-GaN extension region demonstrate a significant decrease in leakage and increase in breakdown voltages. Compared with mesa termination, the optimized HP treatment is also superior due to its low damage without etching. These results can serve as an important reference for future development of plasma-based termination technology in power electronics.

## Data availability statement

All data that support the findings of this study are included within the article (and any supplementary files).

## Acknowledgments

This work was supported by the ARPA-E PNDIODES Program monitored by Dr Isik Kizilyalli and partially supported by the NASA HOTTech Program Grant No. 80NSSC17K0768. The device fabrication was performed at the Center for Solid State Electronics Research at Arizona State University. Access to the NanoFab was supported, in part, by NSF Contract No. ECCS1542160.

## ORCID iDs

Chen Yang https://orcid.org/0000-0002-3009-0882
Kai Fu https://orcid.org/0000-0002-9405-7512
Tsung-Han Yang https://orcid.org/0000-0002-5071-1420

## References

[1] Zhang Y, Sun M, Piedra D, Hu J, Liu Z, Lin Y, Gao X, Shepard K and Palacios T 2017 1200 V GaN vertical fin power field-effect transistors *2017 IEEE Int. Electron Devices Meeting (IEDM)* pp 9.2.1–4
[2] Zhang Y, Sun M, Liu Z, Piedra D, Hu J, Gao X and Palacios T 2017 Trench formation and corner rounding in vertical GaN power devices *Appl. Phys. Lett.* **110** 193506
[3] Amano H *et al* 2018 The 2018 GaN power electronics roadmap *J. Phys. D: Appl. Phys.* **51** 163001
[4] Nomoto K *et al* 2015 GaN-on-GaN p–n power diodes with 3.48 kV and 0.95 m$\Omega$ cm$^2$: a record high figure-of-merit of 12.8 GW cm$^{-2}$ *Tech. Dig.—Int. Electron Devices Meeting IEDM* (*February 2016*) pp 9.7.1–4
[5] Shurrab M and Singh S 2020 Implantation-free edge termination structures in vertical GaN power diodes *Semicond. Sci. Technol.* **35** 65005
[6] Ohta H, Asai N, Horikiri F, Narita Y, Yoshida T and Mishima T 2020 Two-step mesa structure GaN p–n diodes with low ON-resistance, high breakdown voltage, and excellent avalanche capabilities *IEEE Electron Device Lett.* **41** 123–6
[7] Fukushima H, Usami S, Ogura M, Ando Y, Tanaka A, Deki M, Kushimoto M, Nitta S, Honda Y and Amano H 2019 Deeply and vertically etched butte structure of vertical GaN p–n diode with avalanche capability *Japan. J. Appl. Phys.* **58** SCCD25
[8] Zhang Y *et al* 2015 Origin and control of OFF-state leakage current in GaN-on-Si vertical diodes *IEEE Trans. Electron Devices* **62** 2155–61
[9] Sugimoto M, Kanechika M, Uesugi T and Kachi T 2011 Study on leakage current of p–n diode on GaN substrate at reverse bias *Phys. Status Solidi* c **8** 2512–4
[10] Sun Y, Kang X, Zheng Y, Wei K, Li P, Wang W, Liu X and Zhang G 2020 Optimization of mesa etch for a quasi-vertical GaN Schottky barrier diode (SBD) by inductively coupled plasma (ICP) and device characteristics *Nanomaterials* **10** 657
[11] Yoshino M, Sugamata K, Ikeda K, Nishimura T, Kuriyama K and Nakamura T 2019 Ion implanted GaN MISFETs fabricated in Mg implanted layers activated by conventional rapid thermal annealing *Nucl. Instrum. Methods Phys. Res.* B **449** 49–53
[12] Shi Y-T *et al* 2019 Realization of p-type gallium nitride by magnesium ion implantation for vertical power devices *Sci. Rep.* **9** 8796
[13] Niwa T, Fujii T and Oka T 2017 High carrier activation of Mg ion-implanted GaN by conventional rapid thermal annealing *Appl. Phys. Express* **10** 91002
[14] Tsou C, Ji M, Bakhtiary-Noodeh M, Detchprohm T, Dupuis R D and Shen S 2019 Temperature-dependent leakage current characteristics of homojunction GaN p–i–n rectifiers using ion-implantation isolation *IEEE Trans. Electron Devices* **66** 4273–8
[15] Han S, Yang S and Sheng K 2018 High-voltage and high $I_{ON}/I_{OFF}$ vertical GaN-on-GaN Schottky barrier diode with nitridation-based termination *IEEE Electron Device Lett.* **39** 572–5
[16] Fu H, Fu K, Huang X, Chen H, Baranowski I, Yang T, Montes J and Zhao Y 2018 High performance vertical GaN-on-GaN p–n power diodes with hydrogen-plasma-based edge termination *IEEE Electron Device Lett.* **39** 1018–21
[17] Fu H *et al* 2019 Implantation- and etching-free high voltage vertical GaN p–n diodes terminated by plasma-hydrogenated p-GaN: revealing the role of thermal annealing *Appl. Phys. Express* **12** 51015
[18] Fu H *et al* 2020 High voltage vertical GaN p–n diodes with hydrogen-plasma based guard rings *IEEE Electron Device Lett.* **41** 127–30
[19] Ji D, Li S, Ercan B, Ren C and Chowdhury S 2020 Design and fabrication of ion-mplanted moat etch termination resulting in 0.7 m$\Omega$ cm$^2$/1500 V GaN diodes *IEEE Electron Device Lett.* **41** 264–7
[20] Yang C *et al* 2020 Demonstration of GaN-based metal-insulator-semiconductor junction by hydrogen plasma treatment *Appl. Phys. Lett.* **117** 052105
[21] Nomoto K, Song B, Hu Z, Zhu M, Qi M, Kaneda N, Mishima T, Nakamura T, Jena D and Xing H G 2016 1.7 kV and 0.55 m$\Omega$ cm$^2$ GaN p–n diodes on bulk GaN substrates with avalanche capability *IEEE Electron Device Lett.* **37** 161–4
[22] Ohta H, Kaneda N, Horikiri F, Narita Y, Yoshida T, Mishima T and Nakamura T 2015 Vertical GaN p–n junction diodes with high breakdown voltages over 4 kV *IEEE Electron Device Lett.* **36** 1180–2
[23] Hatakeyama Y, Nomoto K, Kaneda N, Kawano T, Mishima T and Nakamura T 2011 Over 3.0 GW cm$^{-2}$ figure-of-merit GaN p–n junction diodes on free-standing GaN substrates *IEEE Electron Device Lett.* **32** 1674–6
[24] Nomoto K, Hatakeyama Y, Katayose H, Kaneda N, Mishima T and Nakamura T 2011 Over 1.0 kV GaN p–n junction diodes on free-standing GaN substrates *Phys. Status Solidi* **208** 1535–7
[25] Hatakeyama Y, Nomoto K, Terano A, Kaneda N, Tsuchiya T, Mishima T and Nakamura T 2013 High-breakdown-voltage

and low-specific-on-resistance GaN p–n junction diodes on free-standing GaN substrates fabricated through low-damage field-plate process *Japan. J. Appl. Phys.* **52** 28007

[26] Hu Z, Nomoto K, Song B, Zhu M, Qi M, Pan M, Gao X, Protasenko V, Jena D and Xing H G 2015 Near unity ideality factor and Shockley-Read-Hall lifetime in GaN-on-GaN p–n diodes with avalanche breakdown *Appl. Phys. Lett.* **107** 243501

[27] Kizilyalli I C, Edwards A P, Nie H, Disney D and Bour D 2013 High voltage vertical GaN p–n diodes with avalanche capability *IEEE Trans. Electron Devices* **60** 3067–70

[28] Wang J, Cao L, Xie J, Beam E, McCarthy R, Youtsey C and Fay P 2018 High voltage, high current GaN-on-GaN p–n diodes with partially compensated edge termination *Appl. Phys. Lett.* **113** 23502

[29] Dickerson J R *et al* 2016 Vertical GaN power diodes with a bilayer edge termination *IEEE Trans. Electron Devices* **63** 419–25

[30] Kizilyalli I C, Edwards A P, Aktas O, Prunty T and Bour D 2015 Vertical power p–n diodes based on bulk GaN *IEEE Trans. Electron Devices* **62** 414–22

[31] Yoshizumi Y, Hashimoto S, Tanabe T and Kiyama M 2007 High-breakdown-voltage p–n-junction diodes on GaN substrates *J. Cryst. Growth* **298** 875–8